ELSEVIER

International Journal of Pharmaceutics 210 (2000) 83–95

international journal of pharmaceutics

www.elsevier.com/locate/ijpharm

Inertial sizing of aerosol inhaled from two dry powder inhalers with realistic breath patterns versus constant flow rates

W.H. Finlay *, M.G. Gehmlich

Aerosol Research Laboratory of Alberta (ARLA), Department of Mechanical Engineering, University of Alberta, Edmonton, Alta., Canada T6G 2G8

Received 8 October 1999; received in revised form 25 August 2000; accepted 28 August 2000

Abstract

A procedure is developed that allows particles inhaled with realistic breath patterns to be sized by cascade impaction at a constant flow rate. This procedure is then used to examine the difference between particle sizes obtained with constant flow rate (step profile) versus actual-subject breath patterns for two dry powder inhalers DPIs; the Ventodisk® and Spiros® inhalers (delivering salbutamol sulphate). Aerosol inhaled from the DPIs by a breath simulator was combined with make-up air to provide 300 l/min. to a pair of virtual impactors. These impactors separate out particles in the nominal diameter range of 1–10 μm for sizing at 30 l/min. by a MOUDI cascade impactor, with filter collection of particles outside this range. Breathing patterns of ten subjects ranging in age from 6 to 17 years of age were measured and recorded using whole-body plethysmography while these volunteers inhaled through Ventodisk® and Spiros® inhalers. Particle sizes with four of these breath patterns, as well as several constant flow rate step profiles, were then obtained using the sizing apparatus with a realistic mouth–throat intake. Our results show that as long as the constant flow rates were near typical values occurring in the actual-subject breaths, particle sizes obtained with constant flow rates were not significantly different ($P > 0.01$) from those occurring with actual-subject breath patterns. Significant differences are present if constant flow rates unrepresentative of those expected during particle uptake with the actual-subject patterns are used with the Ventodisk®. These results show that judiciously chosen constant flow rates give rise to inertial particle size measurements that are equivalent to those obtained during actual-subject inhalation for the two types of DPIs tested.

Keywords: Cascade impaction; Particle size; Powder; Aerosol

1. Introduction

Dry powder inhalers DPIs are a commonly used method of delivering therapeutics to the lung via inhaled aerosols. Because aerosol particle sizes

* Corresponding author. Tel.: +1-403-4924707; fax: +1-403-4922200.

E-mail address: warren.finlay@ualberta.ca (W.H. Finlay).

0378-5173/00/$ - see front matter
PII: S0378-5173(00)00569-X

must be in a relatively narrow range (typically 1–5 μm) in order to provide efficient delivery to the lung, knowledge of the particle sizes produced by powder inhalers is useful, particularly in preclinical assessment of powder formulations (Hickey, 1996). Inertial measurement methods, such as cascade impaction, are commonly used to determine the sizes of powder particles inhaled from DPIs because such methods are relatively inexpensive and easy to use, and allow ready distinction between active ingredients and excipients (by chemical assay of the impacting powder) (Mitchell and Nagel 1997). Indeed, inertial impaction is the only aerosol particle sizing method invoked in pharmacopial formulation testing requirements for dry powder inhaler DPI aerosols.

All the existing inertial sizing methods operate by drawing the aerosol and air through an apparatus at a fixed flow rate. The requirement of a constant 'inhalation' flow rate has been viewed as a principle drawback of these methods (Burnell et al., 1998), since patients using a DPI instead supply a time-varying flow rate through the device, not a constant flow rate. Since powder uptake and deaggregation can be flow rate dependent, it has been argued that inertial sizing methods with constant flow rates may not properly mimic ex vivo operation of DPIs, bringing into question the clinical relevance of such particle size measurements (Brindley et al., 1994).

In order to overcome the fixed flow rate restriction of inertial sizing methods and allow more accurate simulation of patient use of inhalers, various approaches have been developed for DPIs (Lee et al., 1996; Burnell et al., 1998), as well as with metered dose inhalers with holding chambers (Finlay, 1998) and for nebulizers (Finlay et al., 1997). However, these approaches add considerable complexity to the testing apparatus and thereby remove one of the principal attractions of fixed flow rate inertial methods: they are simple to use. For this reason, it is worth examining the error in particle size measurements that may be incurred when using a fixed flow rate versus actual patient inhalation patterns with DPIs, since if these errors are relatively minor then the much simpler use of fixed flow rates is attractive. In the present work, we examine this issue for two different DPIs, the Spiros® and the Ventodisk® (Diskhaler®).

2. Materials and methods

Particle size distributions were measured for salbutamol aerosolized by a Spiros® inhaler supplied by the manufacturer (each actuation delivers salbutamol sulphate equivalent to 90 μg salbutamol per dose, Dura Pharmaceuticals, San Diego, CA) and a Ventodisk® (Ventolin® Diskhaler®) inhaler (each actuation delivers salbutamol sulphate equivalent to 200 μg salbutamol per dose, Glaxo Canada Inc., Toronto, ON) purchased at a local pharmacy. Both inhalers contained lactose as excipient.

2.1. Inertial sizing

A MOUDI cascade impactor (MSP Corp., Minneapolis, MN) was used to measure particle size distributions. To further increase the resolution of the particle sizes expected with the inhalers used in this study, the 0.18 and 0.32 μm stages of this impactor were removed and custom-made stages (MSP Corp., Minneapolis, MN) with nominal cut-points of 4.4 and 6.9 μm were added. The calibrated cut points of the stages of this impactor were thus at 0.524, 1.0, 1.8, 3.2, 4.4, 6.2, 6.9, 9.9 and 18 μm, corresponding to stages eight through zero respectively. The impactor was operated at its designed 30 l/min. flow rate. This flow rate was calibrated using a dry gas meter (DTM-115, American Meter Co., Nebraska City, NE).

In order to allow arbitrary, time-dependent flow rates to occur through the inhalers while the aerosol was collected and sized through the cascade impactor at a constant flow rate, the apparatus shown in Figs. 1 and 2 was used. Briefly, this apparatus combines the inhaler air stream with makeup air to supply a constant flow rate of 300 l/min. to a pair of virtual impactors that separate out particles in the 1–10 micron range for detailed sizing at 30 l/min. with a cascade impactor. For the sake of brevity, this Cascade and Virtual Impactor Combination, shown in Fig. 2, will be referred to by the acronynm CAVIC.

Fig. 1 shows the apparatus that connects the breath simulator through the inhaler to the CAVIC. To allow different breathing patterns to occur through the inhalers, an in-house breath

simulator (Finlay and Zuberbuhler, 1999) was used, connected via flexible plastic tubing to the inhaler enclosure. The breath-simulator uses a computer-controlled stepper motor to drive a piston in a cylinder, thereby supplying the desired time-dependent breath pattern. In the configuration shown in Fig. 1, the breath simulator 'pushes' air through the DPI in order to allow downstream collection of the aerosol via the apparatus in Fig. 2. The inhaler enclosure seals the inhaler in the positive pressure environment supplied by the breath simulator. Because the flow is isothermal, well below Mach numbers of 0.3, and not exposed to large pressure drops in the flow circuit, compressibility effects are negligible so that only pressure changes, and not absolute pressures, are relevant (Panton, 1996). Thus, using positive pressure to 'push' air through the inhaler is identically equivalent to the actual clinical situation where patients 'pull' air through the inhaler via negative pressure.

Downstream of the inhaler, a fiberglass mouth–throat geometry described in Stapleton et al. (1999) that closely mimics the principal features of in vivo mouth–throat geometries was used. This allowed the generated aerosol to be exposed to fluid motions, and particularly turbulence, like that expected in the mouth and throat of actual subjects. Turbulence generated in the inhaler and mouth–throat could affect particle deaggregation. Since such turbulence is flow rate dependent, it could affect particle sizes differently for different inhalation waveforms. In addition, it is the particle size inhaled into the lung that is of most interest in clinical applications, and we wanted to make our comparisons of particle sizes between different inhalation waveforms on this basis, rather than directly at the exit of the inhaler. For these reasons, we have included the mouth–throat assembly as shown in Fig. 1. To prevent particle bounce in the mouth–throat assembly and on the impactor stages, a thin coating of silicone spray (# 316 Silicone Release Spray, Dow Corning, Midland, MI) was used.

Downstream of the mouth–throat assembly, the arbitrary (and time-dependent) flow rate from

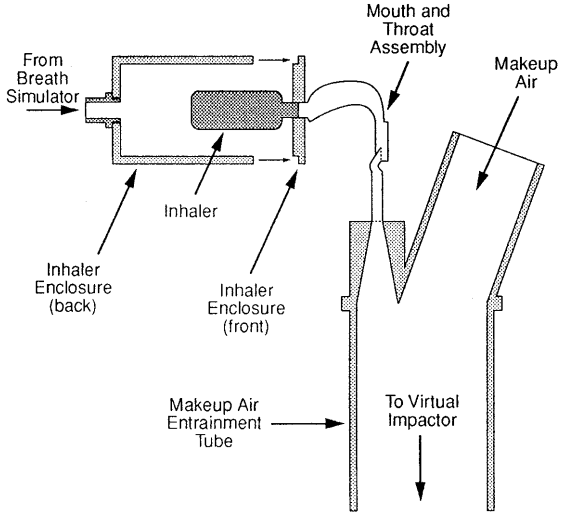

Fig. 1. A schematic of the apparatus used to connect the inhaler to the CAVIC intertial sizing equipment that allows arbitrary flow rates to occur through the inhaler via a breath simulator.

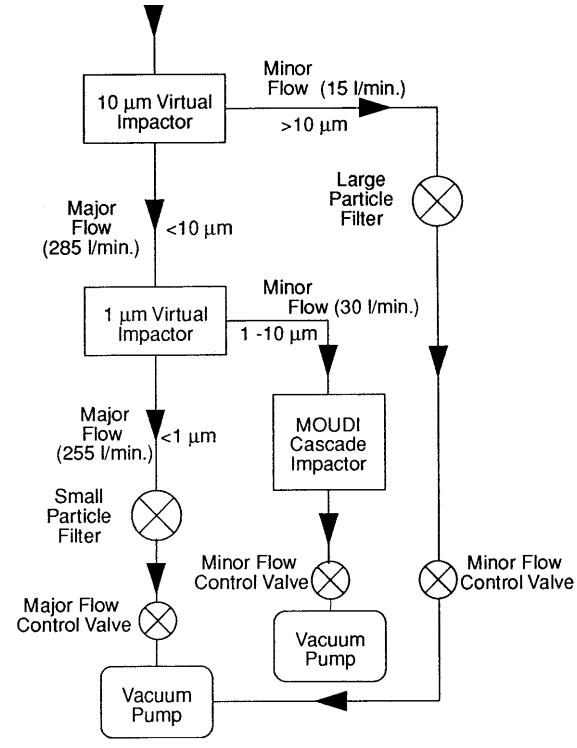

Fig. 2. Flow diagram of the cascade and virtual impactor combination (CAVIC) used to collect the aerosol supplied by the apparatus in Fig. 1.

the inhaler was combined with make-up air via a large diameter opening to ambient air as shown in Fig. 1. In order to avoid production of turbulence in combining these two streams, expansion of the mouth–throat assembly occurred via an expansion cone of shallow angle (7.1° from centerline) and the makeup tube joined the inhaler stream in a nearly parallel manner. In addition, the diameter of the makeup tube (4″ inner diameter) and the inhaler stream (2″ inner diameter) at their joining (6″ inner diameter) was designed such that average flow velocities in the two streams would be equal for typical velocities expected in these two streams, thereby reducing as much as possible the presence of turbulent shear layers between these two streams. The makeup air and inhaler air streams combine to make a constant flow rate of 300 l/min. that enters the virtual impactor arrangement shown in Fig. 2. The design flow rate of 300 l/min. at the intake of the first virtual impactor requires that instantaneous inhalation flow rates through the inhaler are below 300 l/min.

The virtual impactors and their flow control apparatus shown in Fig. 2 were custom modifications of a commercially available atmospheric sampling unit (Universal Air Sampler, model 310c, MSP Corp., Minneapolis, MN). In particular, the cut-point of the downstream virtual impactor was 1.0 μm (instead of 2.5 μm in the stock model) and the design minor flow rate was 30 l/min. (instead of 15 l/min.). In addition, a filter (#303, Marquest Medical Products, Englewood, CO) was placed in the minor flow of the 1st virtual impactor stage (which has a calibrated cut-point of 10 μm). All major and minor flow rates through the virtual impactors were adjusted and continuously monitored using calibrated differential pressure gauges and flow meter orifices supplied with the Universal Air Sampler. The pressure gauge for the minor flow rate of the 1.0 μm virtual impactor was recalibrated for a 30 l/min. reading using the same dry gas meter used to calibrate the cascade impactor flow rate.

The use of the virtual impactor apparatus in Fig. 2 allows division of the aerosol into three nominal size ranges; >10, 1–10 and <1 μm. The middle of these three size ranges is of most interest for inhaled pharmaceutical aerosols. The flow rate of the stream containing 1–10 μm particles was here designed to be 30 l/min., allowing collection of this stream onto the MOUDI impactor for further size resolution, (although this flow rate is readily adjusted to 28.3 l/min. for use with an Anderson impactor).

For the purpose of particle size presentation, amounts of aerosol determined to be in the >10 μm virtual impactor stream were combined with amounts determined to be in the two largest particle stages of the MOUDI impactor (the 9.9 and 18 μm stages) to yield a single amount considered to consist of particles >9.9 μm in diameter. In addition, amounts of aerosol collected in the <1 μm virtual impactor stream were added to amounts determined to be on the cascade impactor stages $k=6$, 7, 8 (which have cut-points 1.8, 1.0, 0.524 μm) and the filter using the equation

$$m_k = \left(1 + \frac{m^{vi}}{\eta_k \sum_{j=6}^{9} m_j^{ci}/\eta_j}\right) m_k^{ci} \quad \text{for } k = 6-9 \qquad (1)$$

Here, m^{vi} is the mass of drug collected on the small particle virtual impactor filter (nominally <1 μm), m_k^{ci} is the mass of drug collected on stage k of the cascade impactor, η_k is the measured efficiency (from the manufacturer's calibration data) of the 1 μm virtual impactor at the cut-point of the kth cascade impactor stage, and m_k is the total amount of drug (from both the virtual and cascade impactor) considered to be in the particle size range of the kth cascade impactor stage. The filter on the cascade impactor is labeled as stage 9 in Eq. (1). The use of Eq. (1) gives a first order approximation to the inversion problem associated with the use of the 1 μm virtual impactor (with its nonideal efficiency curve) upstream of the cascade impactor.

Amounts of drug depositing in the various locations were determined by washing with distilled water and subsequent UV spectrophotometric assay (model 8452A, Hewlett-Packard, Mississauga, ON) at 224 nm. Unless otherwise specified, three doses of drug were collected in each run prior to an assay, and a total of five runs were done for

each flow rate/device combination. Estimates of mass median diameter (MMAD) and geometric standard deviation (GSD) for the measured particle size distributions were obtained by linear interpolation. Statistical analysis of the results was done using ANOVA (using SYSTAT, SYSTAT Inc., Evanston, IL), with Tukey HSD multiple means comparisons. Differences were deemed significant at a P-value of 0.01, unless otherwise stated.

2.2. Validation of CAVIC testing

Prior to using the CAVIC apparatus to examine particle sizes with actual breath patterns, a series of validation tests were done. These tests had two purposes; (1) to ensure that the CAVIC did not significantly alter the particle size distribution and (2) to ensure that overloading of the cascade impactor stages were not occurring. The former effect would be a concern if significant deaggregation, agglomeration, or significant size-dependent losses occurred in the CAVIC, while the latter could result in incorrect sizing as a result of particle bounce, reentrainment and subsequent collection on smaller stages of the cascade impactor.

Examination of overloading was done by collecting aerosol directly onto the MOUDI impactor from the fiberglass mouth–throat (i.e. without the CAVIC) at a constant flow rate of 30 l/min. supplied by a vacuum pump. Overload testing with the Ventodisk® was done by obtaining particle size distributions with two versus three doses per run, while for the Spiros® this was checked by comparing three versus. six doses per run. Five runs were made for each case.

Examination of possible size distribution alterations caused by comparing particle size distributions obtained using the CAVIC (with a constant flow rate of 30 l/min occurring through the inhaler) with those obtained by collecting aerosol directly into the MOUDI impactor from the fiberglass mouth–throat (i.e. without the CAVIC) at 30 l/min. These measurements were done with three doses per run. Five runs were made for each case.

In all these validation tests the constant flow rate of 30 l/min was maintained through the inhaler for 10 s (by disconnecting the inhaler from the vacuum line after this time if using the MOUDI impactor without the CAVIC, or by specifying a fixed inhalation volume with the breath simulator if using the CAVIC).

Results of the validation tests for the Spiros® inhaler showed no significant differences between MMAD, GSD or cumulative amounts on each impactor stage ($P > 0.01$), both for the overloading tests comparing three versus six doses, and for the tests comparing the use of the CAVIC versus direct use of the MOUDI impactor. Similar results were found with the Ventodisk® validation tests. These results indicate that overloading is not significant and that the CAVIC does not significantly alter the inhaled particle size distributions.

2.3. Breath patterns

Actual patient breath patterns measured with subjects while inhaling (without drug delivery) through Spiros® and Ventodisk® inhalers were recorded using an in-house whole-body (head-out) plethysmograph. A pressure transducer (CD15, Validyne Engineering Corp., Northridge, CA) connected to a digital oscilloscope (TDS 410A, Tektronix, Wilsonville, OR) was used to record the pressure in the plethysmograph at a sampling rate of 100 Hz. A calibration syringe was used with each subject to determine the relation between pressure and volume in the plethysmograph, allowing determination of the volume of air in each subject's lungs as a function of time during inhalation through the inhaler. Post-study processing of this data allowed determination of the breathing pattern of each individual subject as they inhaled from each inhaler.

Measurements of breath patterns were made for ten individuals (six males, four females) recruited at a pediatric pulmonary clinic. The subjects ranged in age from 6 to 17 years of age, with an average age of 11.8 years. All volunteers were known to have chronic pulmonary disorders or asthma and all had previous experience using inhaler devices. Immediately prior to measurement of the breath patterns for a subject, the

Table 1
Mean (with standard deviation in brackets) of various flow parameters for the 45 measured inhalation flow patterns

Device	Average inhalation flow rate (l/min)	Peak inhalation flow rate (l/min)	Peak acceleration of inhalation flow rate (l/min per s)	Inhaled volume (l)
Ventodisk	91 (39)	162 (68)	282 (166)	1.9 (0.7)
Spiros	21 (9)	41 (26)	86 (56)	1.4 (0.6)

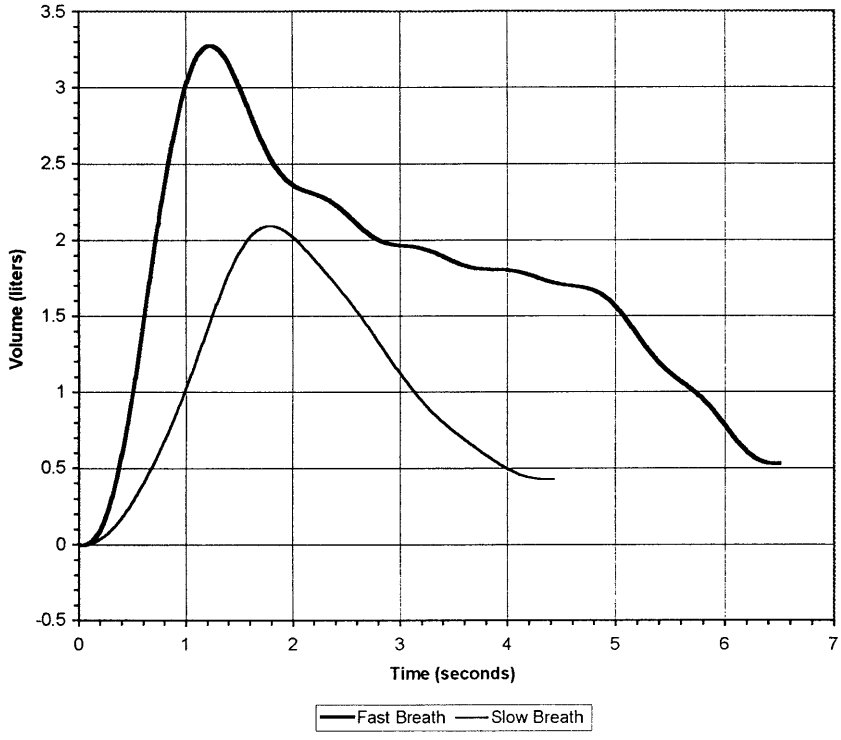

Fig. 3. The two actual-subject breath patterns (patterns 1 and 4 in Table 2) used in testing the Ventodisk® inhaler are shown. Only the inhalation portion of the curve was used. The peak and average inhalation flow rates of the fast breath (pattern 4) are 286 and 165 1/min., respectively, while for the slow breath (pattern 1) they are 117 and 72 1/min. Peak acceleration of flow rate is 485 1/min. per s for the fast breath and 104 1/min. per s for the slow breath.

manufacturers' instructions for proper use of the given inhaler were read and the subject instructed to take several trial breaths through the device to become comfortable with its use. For each individual, at least two breaths were recorded for both a Spiros® and a Ventodisk® inhaler, resulting in the collection of over 40 breath patterns. The mean and standard deviation of various inhalation parameters for the measured patterns are shown in Table 1. After examining peak flow rate, acceleration of the flow rate, and inhaled volume for these patterns, a 'fast' and 'slow' inhalation pattern was chosen for each inhaler to approximately represent the two opposite ends of the range of values observed for these parameters. The fast and slow inhalation patterns are shown in Fig. 3 for the Spiros®, and Fig. 4 for the Ventodisk®. Average and peak flow rates, as well as flow accelerations, of these breath patterns are given in the Figs. 3 and 4. The differences between the breath patterns with these two inhalers was expected, since the Ventodisk® instructions call for a quick, deep breath, while the Spiros® instructions call for a prolonged, slow, steady breath.

Particle sizes obtained with the slow and fast breath patterns shown in Figs. 3 and 4 were obtained using the CAVIC. In addition, particle sizes obtained with several 'square' or 'step' inhalation patterns (i.e. constant inhalation flow rates with abrupt start and finish) using the CAVIC were also obtained. For the Ventodisk®, particle size measurements at constant flow rates corresponding to the peak and average inhalation flow rates of the slow pattern, as well as the average flow rate of the fast pattern and 100 l/min. were made (the latter flow rate being used since the peak inhalation flow rate of the fast pattern exceeded the capabilities of our breath simulator and because 100 l/min is the value suggested in USP guidelines for a low resistance inhaler like the Ventodisk®). For the Spiros® inhaler, particle size measurements were made at constant flow rates corresponding only to the average inhalation flow rate of the slow and fast patterns, since measured inhalation flow rates were relatively independent of time during inhalation with this inhaler. The various breath patterns, including the volumes of inhalation, are summarized in Tables 2 and 3.

Ambient conditions during testing were 23 ± 20°C and 40 ± 10% RH. A single drug lot was used for all Spiros® runs, while two drug lots were used with the Ventodisk, one for all the validation runs and one for all the breath simulation runs.

3. Results

Table 4 shows amounts collected in different regions (the CAVIC, the mouth–throat and remaining in the device), after inhalation with the six different breath patterns used with the

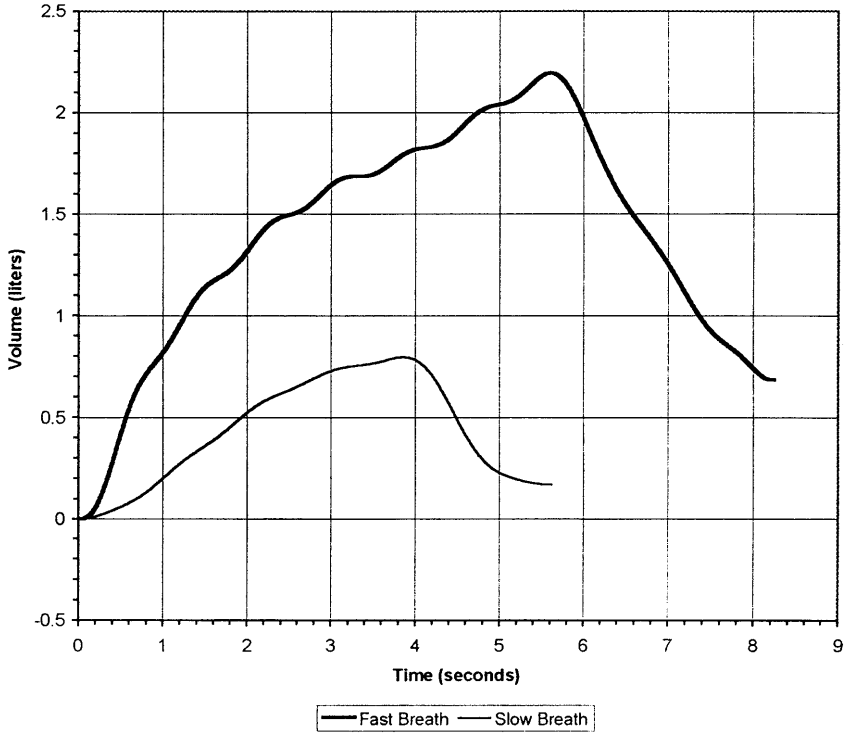

Fig. 4. The two actual-subject breath patterns used in testing the Spiros® inhaler (patterns 7 and 9 in Table 3). Only the inhalation portion of the curve was used. The peak and average flow rates of the fast breath (pattern 9) are 85 and 24 1/min, respectively, while for the slow breath (pattern 7), they are 22 and 12 l/min. for the slow breath (pattern 7). Peak acceleration of flow reate is 203 l/min. per s for the fast breath and 23 1/min per s for the slow breath.

Table 2
The different breath patterns used to measure inhaled particle sizes with the CAVIC when testing the Ventodisk® inhaler

Breath pattern	Flow rate (l/min)	Volume (l)	Description
1	Variable	2.09	Actual-subject slow pattern from Fig. 3
2	72	2.09	Constant flow rate (step profile) corresponding to average inhalation flow rate of pattern 1
3	117	2.09	Constant flow rate (step profile) corresponding to peak inhalation flow rate of pattern 1
4	Variable	3.28	Actual-subject fast pattern from Fig. 3
5	165	3.28	Constant flow rate (step profile) corresponding to average inhalation flow rate of pattern 4
6	100	3.28	Constant flow rate (step profile) corresponding to USP testing of low resistance inhaler

Table 3
The different breath patterns used to measure inhaled particle sizes with the CAVIC when testing the Spiros® inhaler

Breath pattern	Flow rate (l/min)	Volume (l)	Description
7	Variable	0.80	Actual-subject slow pattern from Fig. 4
8	12	0.80	Constant flow rate (step profile) corresponding to average inhalation flow rate of pattern 7
9	Variable	2.20	Actual-subject fast pattern from Fig. 4
10	24	2.20	Constant flow rate (step profile) corresponding to average inhalation flow rate of pattern 9

Table 4
Average amounts ($n = 5$) collected using the Ventodisk® inhaler in the CAVIC, in the mouth–throat, remaining in the inhaler device, and in total with the different breath patterns, given as % label claim, as well as average MMAD and GSD ($n = 5$), are shown with standard deviation in brackets

Breath pattern	CAVIC	Mouth–throat	Device	Total collected	MMAD (μm)	GSD
1	20.5 (4.8)	62.9 (5.3)	17.8 (1.7)	101.2 (2.3)	2.0 (0.2)	1.8 (0.1)
2	18.1 (2.8)	57.0 (2.7)	22.3 (1.8)	97.5 (2.1)	1.9 (0.1)	1.8 (0.1)
3	19.0 (2.0)	63.2 (2.5)	18.3 (1.9)	98.6 (2.5)	1.8 (0.1)	1.7 (0.1)
4	19.8 (2.8)	65.9 (4.4)	14.6 (3.4)	100.3 (2.9)	1.9 (0.1)	1.8 (0.1)
5	19.8 (1.6)	64.2 (3.2)	15.0 (2.2)	98.9 (2.6)	1.7 (0.1)	1.7 (0.1)
6	18.9 (1.9)	62.9 (0.5)	18.2 (1.9)	100.5 (3.3)	1.9 (0.1)	1.7 (0.1)

Table 5
Same as Table 4 but for the Spiros® inhaler

Breath pattern	CAVIC	Mouth–throat	Device	Total collected	MMAD (μm)	GSD
7	14.1 (1.5)	48.6 (4.9)	34.9 (3.6)	97.6 (1.3)	2.1 (0.2)	1.8 (0.1)
8	14.5 (3.9)	48.5 (4.0)	38.5 (3.3)	101.5 (2.8)	2.1 (0.1)	1.8 (0.1)
9	15.9 (3.8)	55.3 (4.3)	29.3 (2.0)	100.5 (3.8)	2.0 (0.1)	1.8 (0.1)
10	14.0 (4.0)	55.8 (4.4)	29.1 (3.5)	98.9 (3.4)	2.2 (0.2)	1.9 (0.3)

Ventodisk® inhaler from Table 2, while Table 5 shows the same information for the four different breath patterns combinations used with the Spiros® inhaler from Table 3. Also shown are MMADs and GSDs. None of the differences in any of the quantities in Table 4 or Table 5 are significant at a p-value of 0.01 when comparing data obtained with actual-subject breath patterns to their associated constant flow rates (i.e. differences within breath patterns 1–3, breath patterns 4–6, breath pattern 7 vs. 8, and breath pattern 9 vs. 10 are not significant).

Between slow and fast types of breaths, significant differences are present ($P < 0.01$). For the Ventodisk®, these differences include a significantly larger MMAD in the CAVIC with the slow actual-subject breath pattern than at a constant flow rate of 165 l/min. (pattern 5), as well as significantly more left drug behind in the inhaler ($P < 0.01$) after inhalation at 72 l/min (pattern 2) than at either 100 l/min. or 165 l/min. (patterns 4 and 5). Similarly, significantly more drug ($P < 0.01$) was left in the Spiros® with the slow actual-subject breath (pattern 8) than either fast breath (pattern 9 or 10).

In comparing the Ventodisk® and Spiros®, differences between Table 3 and Table 4 are significant in MMAD only between pattern 5 (165 l/min) versus patterns 7, 8 or 10. The two inhalers also differ in mouth–throat deposition, where all Ventodisk® breaths except pattern 2 gave significantly more mouth–throat deposition ($P < 0.01$) than either of the two slow Spiros® breaths (patterns 7 and 8) and similarly for the actual-subject Ventodisk® fast breath (pattern 4) versus the two fast Spiros® breaths (patterns 9 and 10).

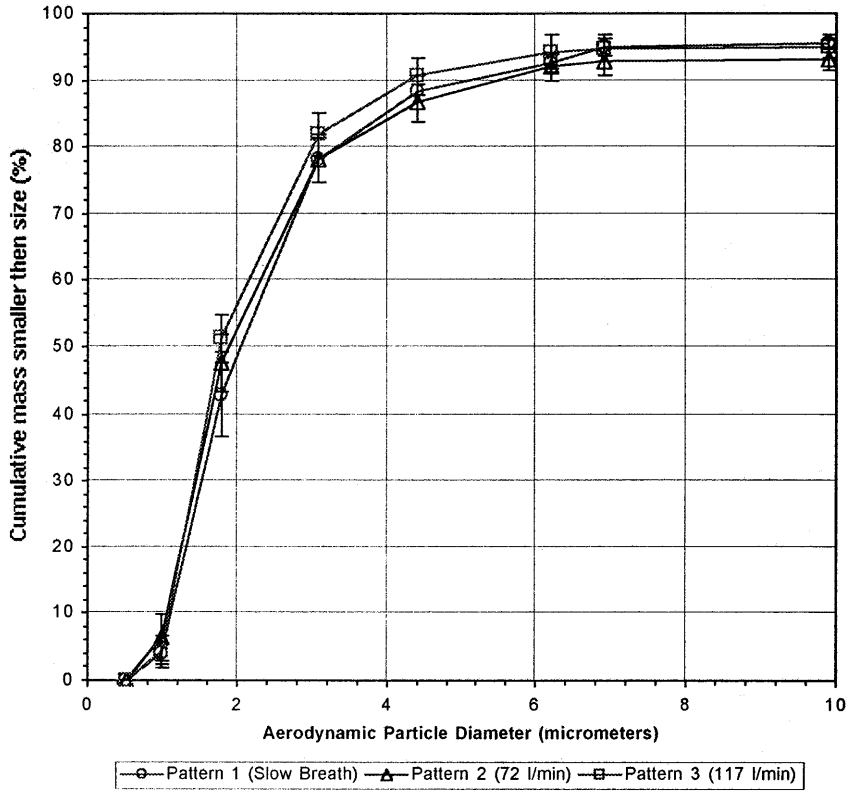

Fig. 5. Particle size distributions distal to the mouth–throat for the Ventodisk® actual-subject slow breath pattern and associated constant flow rates (breath patterns 1–3 in Table 2) are shown are cumulative % less than the size. Error bars show standard deviation (S.D.).

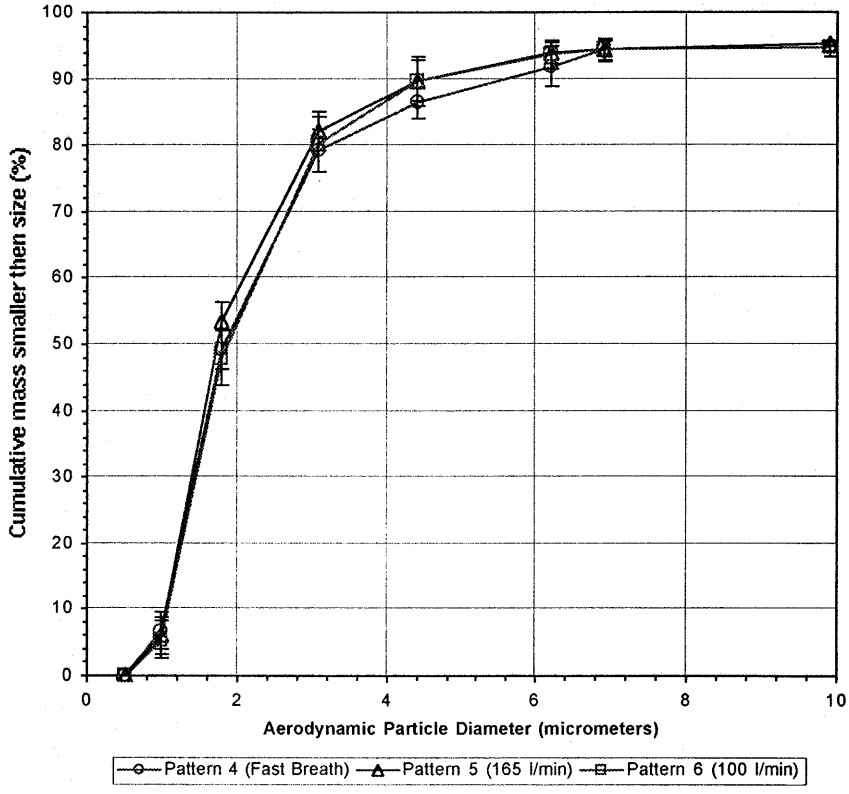

Fig. 6. Particle size distributions distal to the mouth–throat for the Ventodisk® actual-subject fast breath pattern and associated constant flow rates (breath patterns 4–6 in Table 2) are shown as cumulative % less than size. Error bars show S.D.

Cumulative particle size distributions distal to the mouth–throat are shown in Figs. 5–8. In particular, particle size distributions collected in the CAVIC for the actual-subject slow breathing pattern and associated constant flow rates (breath patterns 1–3) are shown in Fig. 5 for the Ventodisk®. Fig. 7 shows similar data for the Spiros®. Particle size distributions for the actual-subject fast breathing patterns and associated constant flow rates are shown in Fig. 6 for the Ventodisk®. Fig. 8 shows similar data for the Spiros®. None of the differences between breath patterns within a given figure are significant ($P > 0.01$) when cumulative percentages in each size range are compared.

4. Discussion

Our results suggest that constant-flow-rate inertial impactors can produce particle sizes that are negligibly different from those obtained with actual-subject breaths (at least for the Spiros® and Ventodisk® inhalers), as long as the impactors are run at flow rates near typical values occurring in the actual-subject breaths.

This conclusion is expected for the Spiros® inhaler, since this 'active' device uses battery-operated spinning impellers to assist particle deaggregation on inhalation, instead of relying totally on patient inhalation for this purpose. Indeed, lung deposition with this device has been found to be relatively insensitive to inhalation flow rate (Hill et al., 1996), which corroborates our observed lack of flow rate dependence with this device.

In contrast, the Ventodisk® relies solely on patient inhalation for powder uptake and deaggregation, and does exhibit flow rate dependent particle size (Ross and Schultz, 1996, Hindle and Byron, 1995), and also observed here with the fast

versus slow breath patterns. However, our results indicate that this flow rate dependence in particle size does not translate into significant differences when constant flow rates are compared to actual-subject breaths that have a similar average flow rate. A possible explanation of this observation can be proposed as follows by considering particle uptake and deaggregation. In particular, with the actual-subject breath patterns, significant particle uptake does not occur until partway into the breath when the flow rate has increased to an appreciable value (Clark and Bailey 1996). Particle deaggregation of the entrained powder then occurs at the instantaneous flow rate associated with uptake, with smaller particle sizes tending to result at higher instantaneous flow rates. Examining Fig. 3, it can be seen that the instantaneous flow rate (which is the slope of the volume vs. time curve shown there) is relatively constant (and is near the average inhalation flow rate) once the flow rate reaches an appreciable value. Thus, when a step profile is used with a constant flow rate that is near the average inhalation flow rate, powder uptake and deaggregation with the step profile should be similar to that occurring with the actual-subject breath pattern, as is indeed observed in our results with the Ventodisk®.

This explanation also suggests that when a step profile is used with flow rate that differs considerably from that occurring during powder uptake in the actual-subject breath pattern, it is reasonable to expect different powder deaggregation and subsequently different particle sizes, as is also observed in our results with the Ventodisk® [differences are notable in MMAD for two situations with the Ventodisk® in Table 4; at 165 vs. 100 l/min. (i.e. pattern 5 vs. pattern 6 gives $P = 0.043$), as well as with the actual-subject slow

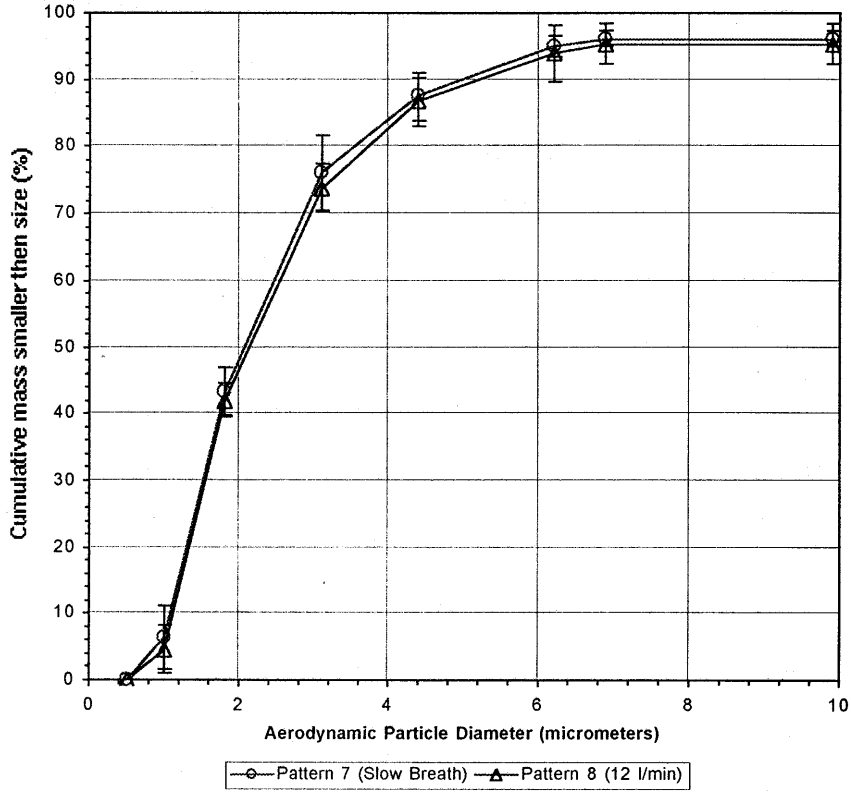

Fig. 7. Particle size distributions distal to the mouth–throat for the Spiros® actual-subject slow breath pattern and associated constant flow rate (breath patterns 7 and 8 in Table 3) are shown as cumulative % less than size. Error bars show S.D.

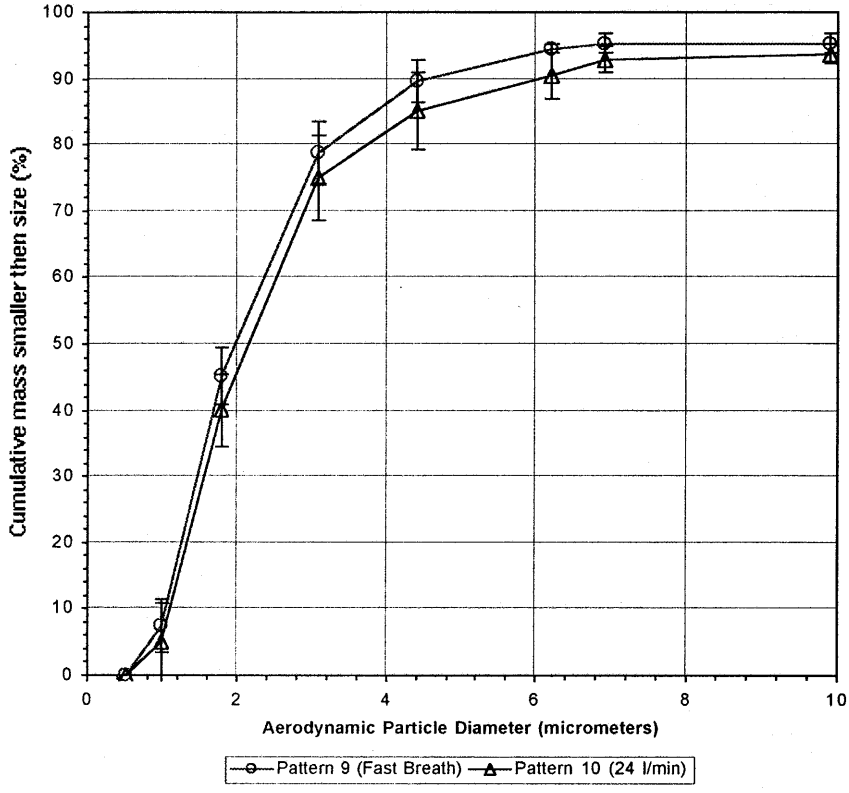

Fig. 8. Particle size distributions distal to the mouth–throat for the Spiros® actual-subject fast breath pattern and associated constant flow rate (breath patterns 9 and 10 in Table 3) are shown as cumulative % less than size. Error bars show S.D.

pattern vs. its peak flow of 117 l/min (i.e. pattern 1 vs. 3 gives $P = 0.048$)]. Because the Spiros® inhaler uses a spinning impeller (driven by a battery) to assist deaggregation, this same explanation suggests that particle size with the Spiros® should be less dependent on the flow rate at which powder uptake occurs, as is seen in our results.

The above discussion ignores possible effects due to the flow rate and particle size dependence of deposition in the mouth–throat. However, our results do not show significant differences in mouth–throat deposition between the different breath patterns for each inhaler. Thus, changes in mouth–throat deposition do not appear to be primarily responsible for our observed flow rate effects in a given inhaler. However, it is interesting to note the differences in mouth–throat deposition between the Spiros® and Ventodisk®. The latter has higher mouth–throat deposition, presumably due to impaction caused by the much higher flow rates associated with the low resistance of this device.

The conclusion that inertial size measurements with a constant flow rate can adequately reproduce particle sizes occurring with realistic breath patterns (as long as flow rates similar to those expected in the realistic breaths during particle uptake are used) is important because it provides support for the use of much simpler, constant flow rate, in vitro testing. Whether this conclusion applies to DPIs other than those considered here remains for future research.

Acknowledgements

The laboratory and technical help of H. Orszanska, D. Jones, C. Shute, B. Faulkner, T. Gear, B. Hennig and the financial support of the Alberta Lung Association, the Natural Science and Engineering Research Council and Dura Pharmaceuticals, is gratefully acknowledged.

References

Brindley, A., Reavill, K.J., Sumby, B.S., Smith, I.J., 1994. The in-vitro characterization of inhalation devices using the electronic lung™. In: Byron, P.R., Dalby, R.N., Farr, S.J. (Eds.), Resp. Drug Delivery IV. Interpharm Press, Buffalo Grove, IL.

Burnell, P.K.P., Malton, A., Reavill, K., Ball, M.H.E., 1998. Design, validation and initial testing of the electronic lung™ device. J. Aerosol. Sci. 29, 1011–1025.

Clark, A.R., Bailey, R., 1996. Inspiratory flow profiles in disease and their effects on the delivery characteristics of dry powder inhalers. In: Dalby, R.N., Byron, P.R., Farr, S.J. (Eds.), Resp. Drug Delivery V. Interpharm Press, Buffalo Grove, IL.

Finlay, W.H., 1998. Inertial sizing of aerosol inhaled during pediatric tidal breathing from an MDI with attached holding chamber. Int. J. Pharm. 168, 147–152.

Finlay, W.H., Zuberbuhler, P., 1999. In vitro comparison of beclomethasone and salbutamol MDI aerosols inhaled during pediatric tidal breathing from four valved holding chambers. Chest 114, 1676–1680.

Finlay, W.H., Stapleton, K.W., Zuberbuhler, 1997. Predicting lung dosages of a nebulized suspension: Pulmicort® (Budesonide). Particulate Sci. Tech. 15, 243–251.

Hill, M., Vaughan, L., Dolovich, M., 1996. Dose targeting for dry powder inhalers. In: Dalby, R.N., Byron, P.R., Farr, S.J. (Eds.), Resp. Drug Delivery V. Interpharm Press, Buffalo Grove, IL, pp. 197–208.

Hickey, A.J., 1996. In: Hickey, A.J. (Ed.), Inhalation Aerosols. Marcel Dekker, New York.

Hindle, M., Byron, P.R., 1995. Dose emissions from marketed dry powder inhalers. Int. J. Pharm. 116, 169–177.

Lee, K.C., Suen, K.O., Yianneskis, M., Marriott, C., 1996. Investigation of the aerodynamic charateristics of inhaler aerosols with an inhalation simulation machine. Int. J. Pharm. 130, 103–113.

Mitchell, J.P., Nagel, M.W., 1997. Medical aerosols: techniques for particle size evaluation. Particulate Sci. Tech. 15, 217–241.

Panton, R.L., 1996. Incompressible Flow. Wiley, New York.

Stapleton, K.W., Guentsch, E., Hoskinson, M.K., Finlay, W.H., 1999. On the suitability of k-ε turbulence modelling for aerosol deposition in the mouth and throat: a comparison with experiment. J. Aerosol Sci. 31, 739–749.